Antibacterial Electrospun Polycaprolactone Membranes Coated with Polysaccharides and Silver Nanoparticles for Guided Bone and Tissue Regeneration

Davide Porrelli,* Mario Mardirossian, Luigi Musciacchio, Micol Pacor, Federico Berton, Matteo Crosera, and Gianluca Turco

ABSTRACT: Electrospun polycaprolactone (PCL) membranes have been widely explored in the literature as a solution for several applications in tissue engineering and regenerative medicine. PCL hydrophobicity and its lack of bioactivity drastically limit its use in the medical field. To overcome these drawbacks, many promising strategies have been developed and proposed in the literature. In order to increase the bioactivity of electrospun PCL membranes designed for guided bone and tissue regeneration purposes, in the present work, the membranes were functionalized with a coating of bioactive lactose-modified chitosan (CTL). Since CTL can be used for the synthesis and stabilization of silver nanoparticles, a coating of this compound was employed here to provide antibacterial properties to the membranes. Scanning electron microscopy imaging revealed that the electrospinning process adopted here allowed us to obtain membranes with homogeneous fibers and without defects. Also, PCL membranes retained their mechanical properties after several weeks of aging in simulated body fluid, representing a valid support for cell growth and tissue development. CTL adsorption on membranes was investigated by fluorescence microscopy using fluorescein-labeled CTL, resulting in a homogeneous and slow release over time. Inductively coupled plasma−mass spectrometry was used to analyze the release of silver, which was shown to be stably bonded to the CTL coating and to be slowly released over time. The CTL coating improved MG63 osteoblast adhesion and proliferation on membranes. On the other hand, the presence of silver nanoparticles discouraged biofilm formation by *Pseudomonas aeruginosa* and *Staphylococcus aureus* without being cytotoxic. Overall, the stability and the biological and antibacterial properties make these membranes a valid and versatile material for applications in guided tissue regeneration and in other biomedical fields like wound healing.

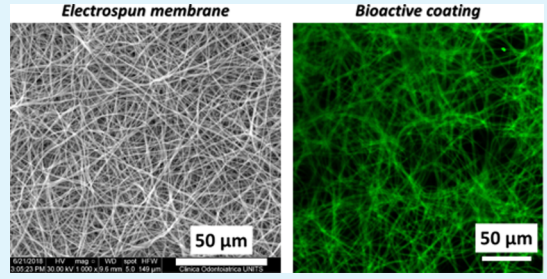

KEYWORDS: *silver nanoparticles, bioactivity, electrospinning, antibacterial, tissue engineering*

1. INTRODUCTION

Guided bone regeneration (GBR) and guided tissue regeneration (GTR) are dental surgical procedures for bone and periodontal ligament regeneration. In these procedures, the use of membranes is imperative to guide the growth of soft tissues and to isolate and maintain the space for bone regeneration.[1−5] Currently, two different types of membranes can be used: nonabsorbable and biodegradable. Nonabsorbable membranes (*i.e.*, expanded or high-density polytetrafluoroethylene embedded in a titanium mesh) are characterized by biocompatibility and high mechanical strength and stability, but they are usually bioinert and their use requires secondary surgical intervention for their removal.[2,6,7] Biodegradable membranes can be prepared using both natural (collagen or gelatin to name some) and synthetic polymers [*e.g.*, polycaprolactone (PCL), polylactic acid, polyglycolic acid, and copolymers]; they are biocompatible and can be modified to introduce bioactive properties (*i.e.*, osteoinductivity and osteoconductivity), but they are characterized by poor mechanical strength and their degradation rate must be carefully regulated.[2,6,8] Electrospun nanofiber-based polymeric membranes can be used for the preparation of medical devices for several applications such as wound healing, surgical wound dressing, and guided tissue regeneration.[2,8,9] The electrospinning (ELS) process allows us to produce nanostructured fibrous membranes whose features could be accurately regulated in terms of the fiber diameter, deposition pattern and architecture, mechanical properties, and degradation rate.[1,8] The architecture of this fibrous nanostructure plays a

paramount role, being similar to the one of the native extracellular matrix. This feature represents a hallmark of these membranes and allows us to consider them as a valid substrate for cell adhesion and proliferation.[5,10,11] Another inherent advantage of nanofibers is their high surface-to-volume ratio, which enables them to functionalize membranes with bioactive and functional components and to use them as drug delivery devices.[10,12−14] Synthetic polymers are the best choice for the ELS of nanofibers as they can be easily solubilized in organic and volatile solvents and can be controlled more straightforwardly than natural polymers (*e.g.*, polysaccharides); thus, the parameters that affect the ELS process, such as viscosity and surface tension, can be easily tuned in a more reliable way.[1] Among synthetic polymers employed for ELS in the biomedical field, PCL is one of the most noteworthy, thanks to its biocompatibility and slow biodegradability.[10,11,15,16] As for other synthetic polymers, one of the main drawbacks of PCL is its intrinsic hydrophobicity, which hampers cell adhesion and spreading.[5,11,17,18] The lack of bioactivity can be overcome by modifying the chemical nature of the membranes or by adding bioactive components on the membranes. Physical and chemical modification of hydrophobic polymers can be performed to increase their hydrophilicity and thus cell adhesion; for this purpose, plasma-cleaning procedures, ozone treatments, and acid etching have been successfully applied to membranes.[17,18] Among these processes, the air−plasma cleaning is simple, cost-effective, and widely used to increase the hydrophilicity of polymeric materials (*e.g.*, poly-ether-ether-ketone, PCL, and polydimethylsiloxane)[19−21] by the introduction of polar groups such as carboxylic ones.[21,22] The addition of bioactive components on the membranes can be performed by chemical bonding or chemical adsorption or by the inclusion of the bioactive factors within the nanofibers during the ELS process.[23,24] For example, polysaccharides can be adsorbed on or bound to membranes,[18] or the polymeric solutions used in the ELS process for the nanofiber production can be loaded with bioactive factors such as nanoparticles.[4,14] Membranes for GBR and GTR applications, based on electrospun nanofibers, have been widely explored in the literature. In these devices, PCL is usually the main component because of the abovementioned advantages and is often combined with gelatin or other polymers in order to increase its bioactivity and modulate its degradation rate.[5,25−27] In the context of bioactive polymer adsorption, lactose-modified chitosan (CTL) is a promising polysaccharide, which can be used to functionalize biomaterials. CTL is derived from the addition of lactose moieties to the chitosan backbone; the structure thus obtained is highly hydrophilic and can be used for the preparation of coatings,[28,29] viscous solutions and hydrogels,[30−32] membranes,[33,34] and nanoparticles.[35] The bioactivity of CTL is mediated by galectins, which are proteins present in the intracellular and extracellular environments that trigger molecular signaling when they bind specific residues as galactose moieties.[36,37] The first evidence of CTL bioactivity was shown for chondrocytes: CTL induces their aggregation and stimulates the synthesis of the extracellular matrix and glycosaminoglycan.[38] Recently, it was shown that lactose-derived chitosan can be used for the preparation of scaffolds for hepatocyte culture[39] and for the preparation of substrates for the stimulation of neuron adhesion and neural network activity.[28] CTL proved to work as a bioactive coating on inert inorganic and organic surfaces and on bio-inert polysaccharides: it proved to positively affect neuron adhesion and function on glass substrates[28] and osteoblast adhesion on methacrylic thermosets[29] and alginate porous scaffolds.[40] Another critical issue in GBR and GTR is the challenging environment offered by the oral cavity, which is highly exposed to infections. The use of antibiotics is the standard procedure, but it represents a global issue due to the development of multidrug-resistant bacteria.[3,41] The recent efforts in the development of electrospun membranes are mainly focalized on the use of antibiotics such as metronidazole, ornidazole, and doxycycline, which can be dissolved in the polymeric solution, grafted on the nanofibers, or loaded within nanoparticles.[3,27,42−44] In the recent years, wide-spectrum antibacterial compounds and strategies have been developed; among them, silver nanoparticles (nAgs) emerged as a valid strategy as they can be easily prepared and included in biomaterials; below a certain concentration level, they are not toxic for the cells; and on the other hand, they exert antibacterial activity without causing the development of resistant bacterial strains.[41,45] nAgs have been used in the preparation of membranes for GTR and GBR applications, and different strategies have been adopted for their incorporation within membranes. nAgs can be added during the process of membrane preparation as reported by Abdelaziz *et al.*[25] for PCL electrospun membranes or by Marques *et al.*[46] for natural rubber-based membranes. nAgs can be also incorporated in membranes by sputtering or sonication as proposed by Chen *et al.*[47] Moreover, nAgs can be prepared directly on the membranes by an *in situ* reduction with dopamine as reported by Qian *et al.* and Wang *et al.*[48,49] CTL can be used for the synthesis and stabilization of nAgs: these are obtained by chemical reduction, mediated by ascorbic acid, of silver ions dispersed in CTL.[50] The resulting modified polymer can be used as an antibacterial coating for biomaterials, which slowly releases silver ions and avoids bacterial adhesion and biofilm formation.[29,40,50,51] The work presented here is focused on the preparation of PCL electrospun membranes functionalized with CTL and nAgs in order to obtain bioactive and antibacterial membranes for GBR and GTR.

2. MATERIALS AND METHODS

2.1. Materials. PCL (M_w: 80,000 Da), dichloromethane (DCM), and *N*,*N*-dimethylformamide (DMF) were purchased from the company Sigma-Aldrich (USA). The D-ES30PN-20W potential generator was purchased from Gamma High Voltage Research Inc. (Ormond Beach, FL, USA). The syringe pump, model KDS-100-CE, was purchased from KD Scientific (Holliston, MA, USA). Fortuna Optima glass syringes (an inner diameter of 9 mm) were purchased from Sigma-Aldrich (USA). Silver nitrate ($AgNO_3$), ascorbic acid ($C_6H_8O_6$), phosphate-buffered saline (PBS), Luria−Bertani (LB) broth, LB Agar, and brain heart infusion were purchased from Sigma-Aldrich (USA). Trypsin/ethylenediaminetetraacetic acid solutions, fetal bovine serum (FBS), penicillin/streptomycin 100×, L-glutamine 100×, and Dulbecco's modified Eagle's medium (DMEM) were purchased from EuroClone (Milan, Italy). All other chemicals were of analytical grade. CTL was provided from BiopoLife (Trieste, Italy); its final composition, determined by means of ^{1}H NMR, resulted to be: glucosamine residue 27%, *N*-acetylglucosamine 18%, and 2-(lactit-1-yl)-glucosamine 55%. The calculated relative M_W of CTL is around 1.5×10^6 Da, as determined by viscosimetry.[52] CTL enriched with nAgs (CTL-nAg) was obtained by reducing silver ions with ascorbic acid in a CTL solution according to Travan *et al.* (2009).[50] Briefly, 4 g/L of CTL was dissolved in deionized water. Silver nitrate ($AgNO_3$) was added to CTL at a final concentration of 1 mM; then, ascorbic

acid was added at a final concentration of 0.5 mM. The solution was kept for 4 h at room temperature in darkness and then stored at 4 °C.

2.2. Preparation of PCL Membranes. PCL 12% w/v was solubilized in DCM/DMF (ratio 7:3), first preparing the solution of PCL in DCM and then adding DMF to the solution. Membranes were obtained after 1 h of the ELS process using the following parameters: flow rate, 0.6 mL/h; voltage, 17 kV; distance between the needle and collector, 25 cm; and needle diameter, 27 G. Membranes were collected on an aluminum foil placed on the collector and were detached from the aluminum foil by immersion in 100% ethanol.

2.3. Scanning Electron Microscopy. Membrane samples were placed on aluminum stubs covered with a carbon double-sided tape. Samples were sputter-coated with gold using a Sputter Coater K550X (Emitech, Quorum Technologies Ltd, UK) and then analyzed by a scanning electron microscope (Quanta 250 SEM, FEI, Oregon, USA) working in a secondary electron detector. The working distance was set at 10 mm to obtain the appropriate magnifications, and the acceleration voltage was set at 30 kV. Fiber diameters were measured using Fiji software.[53]

2.4. Membrane Activation. PCL membranes were subjected to an air−plasma treatment in order to increase their hydrophilicity and to allow CTL adsorption. The process was performed using a PDC-32G plasma cleaner (Harrick Plasma, Ithaca NY, USA) set at low power (6.8 W) for 5 min at an RF frequency of 8−12 MHz.

2.5. Attenuated Total Reflectance−Fourier Transform Infrared Spectroscopy. Attenuated total reflectance−Fourier transform infrared (ATR−FTIR) spectroscopy was performed to analyze the surfaces of the samples. IR spectra were acquired with a Nicolet 6700 spectrometer (Thermo Scientific, MI, Italy) within a wavenumber range of 4000−400 cm^{-1}. Three samples for each condition were analyzed, acquiring the spectrum with 32 scans and a resolution of 4 cm^{-1}.

2.6. X-ray Photoelectron Spectroscopy and Near-Edge X-ray Absorption Fine Structure Spectroscopy. The samples were investigated by a combination of near-edge X-ray absorption fine structure (NEXAFS) and high-resolution X-ray photoemission spectroscopy (XPS) at the CNR-BACH beamline[54] of the ELETTRA Synchrotron light source in Trieste, Italy. C 1s and O 1s XPS spectra were recorded using different photon energies (650 and 860 eV) and a Scienta 3000 electron analyzer. The charging effect due to the low electron conductivity of the samples did not allow us to collect analyzable XPS spectra. NEXAFS spectra at the O K-edge of air−plasma-treated and untreated samples were acquired in the total fluorescence yield mode using a multi-channel plate detector (Hamamatsu F4655-13) with a photon energy resolution of 0.15 eV.

2.7. Contact Angle and Surface Energy Analyses. Membrane hydrophilicity was tested by measuring water contact angles using the sessile drop method. An optical microscope (Leica MZ16) equipped with a digital camera (Leica DFC 320) and a 45° tilted mirror, which allowed us to visualize the profile of the liquid drop deposited on the sample, were used for image acquisition. 4 μL of deionized water was deposited on the sample, and the images were acquired after 30 s to ensure the stabilization of the water drop. Image Pro 3D Suite software was used for image acquisition and processing. In order to facilitate drop imaging on air−plasma-treated membranes, deionized water was stained with 1% methylene blue. Surface energies were measured using the Owens−Wendt method[55] adapted by Ren *et al.*[56] and Can-Herrera *et al.*[21] 4 μL of both deionized water and diiodomethane was used for the measurement of the contact angles, whose values were used for the calculation of the surface energy (γ_s) components: the dispersive/hydrophobic component (γ_s^d) and the polar/hydrophilic component (γ_s^p).

2.8. Confocal Microscopy Analysis of CTL Adsorption on Electrospun PCL Membranes. PCL membranes, untreated or air−plasma-treated, were coated with fluorescein-labeled CTL (CTL-FITC, prepared as reported by Marsich *et al.* 2013[40]). For the adsorption, membrane samples were soaked at room temperature for 2 h in 200 μL of the water solution of CTL-FITC, 2 mg/mL, pH 7.4. After the incubation, the samples were washed with deionized water and mounted on a glass coverslip using Mowiol mounting medium (Sigma-Aldrich). Samples were analyzed with a Nikon Eclipse C1 microscope, equipped with a Nikon Plan Fluor lens (numerical aperture: 2.1, dry), using an argon laser (488 nm) and an acquisition channel at 515−530 nm. The images obtained were analyzed using Fiji software.[53]

2.9. CTL Adsorption and Release Evaluation with Spectrofluorimetry. Air−plasma-treated PCL membranes were coated with CTL-FITC as described above. After the adsorption process, the fluorescence of the CTL-FITC solution was measured in order to determine the amount of adsorbed CTL-FITC. Then, the amount of CTL-FITC released from the membranes in the saline solution was determined at different time points (1, 4, 7, and 10 days) by incubating CTL-FITC-coated membranes in 500 μL of saline solution, changing the solution at each time point, and measuring its fluorescence intensity. Fluorescence intensity measures were obtained with the GloMax Multi+ Detection System spectrofluorometer (Promega, Madison, WI, USA) using an excitation wavelength of 490 nm and collecting the fluorescence emission in the range 510−570 nm.

2.10. CTL-nAg Adsorption and Release Evaluation with Inductively Coupled Plasma−Mass Spectrometry. Air−plasma-treated PCL membranes were coated with CTL-nAg. For the adsorption, membrane samples were soaked at room temperature for 2 h with 200 μL of the water solution of CTL-nAg, 2 mg/mL, pH 7.4. The amount of silver released from the membranes in the saline solution was determined at different time points (1, 2, 3, and 4 days), incubating CTL-nAg-coated membranes in 200 μL of saline solution and changing the solution at each time point. The released solution was added to 100 μL of HNO_3 and then brought up to 5 mL with deionized water. At the end of the experiment, residual silver contained in membranes was measured by dissolving the membranes in 1 mL of a 50% v/v aqueous solution of HNO_3; after the dissolution, 4 mL of deionized water was added. Silver quantification was performed by inductively coupled plasma−mass spectrometry (ICP−MS) using a Nexion 350X spectrometer with an ESI autosampler (PerkinElmer, USA instrument, PerkinElmer, Waltham, Massachusetts, MA, USA). A five-point standard curve obtained by dilution of the Ag standard solution for ICP−MS analysis (by Sigma-Aldrich, Milan, Italy) was used for ICP−MS calibrations (0.01−10 μg/L, ion mass 107 Da). Matrix effects were evaluated by means of laboratory-fortified blanks and laboratory-fortified samples prepared at the Ag concentration of 1 and 5 μg/L and analyzed before and after the samples. The Ag recovery was always higher than 95%. The limit of detection was 0.005 μg/L, and the precision of the measurements as repeatability (relative standard deviation %) for the analysis was lower than 3%.

2.11. Analysis of Mechanical Properties and Stability. Membrane stability was analyzed by measuring weight variations and the mechanical properties of the samples aged in simulated body fluid (SBF) at 37 °C. Samples were cut into a dog bone shape following the ASTM D638-10 guidelines.[57] The SBF was prepared by dissolving NaCl, $NaHCO_3$, KCl, K_2HPO_4, $MgCl_2{\cdot}6H_2O$, $CaCl_2$, and Na_2SO_4 in deionized water and buffering at pH 7.4 with tris(hydroxymethyl)aminomethane $(CH_2OH)_3CNH_2$ and 1.0 M HCl at 36.5 °C.[58] The final ion concentrations are nearly equal to those of human blood plasma (Na^+ 142.0, K^+ 5.0, Mg^{2+} 1.5, Ca^{2+} 2.5, Cl^- 147.8, HCO_3^- 4.2, HPO_4^{2-} 1.0, and SO_4^{2-} 0.5 mM). Weight variations and mechanical properties were assessed after 1, 2, 3, 4, 8, 12, 16, and 20 weeks. Five samples were tested at each time point. The SBF solution was changed every week.

Membrane mechanical properties were analyzed by uniaxial tensile tests using a Dynamic Mechanical Analysis (DMA) system (Electroforce 3300, TA Instruments, New Castle, DE, USA) coupled with a 22 N load cell. Samples were tested using the constant deformation of 1 mm/min until sample failure or up to the maximum displacement allowed by the device (20 mm). Maximum strength and strain, or strain and stress at break, were recorded. In all data, the elastic region was clearly detectable as the linear behavior of the stress−strain curve. Therefore, the elastic modulus of each sample was calculated with a

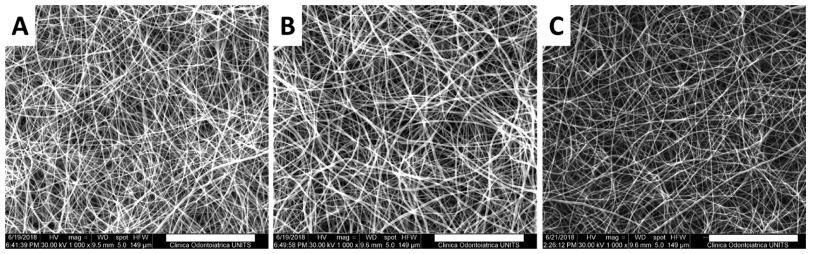

Figure 1. Morphological aspect of the electrospun membranes: (A) untreated PCL membrane; (B) plasma-treated PCL membranes; and (C) air–plasma-treated PCL aged in deionized water for 1 week. The scale bar is 50 μm.

linear fitting of 10–20% range of deformation in the stress–strain curve.

2.12. Cell Culture. Osteosarcoma-derived human osteoblasts (MG63, ATCC code: CRL-1427) were grown in DMEM, supplemented with 10% FBS, penicillin 100 U/mL, streptomycin 0.1 mg/mL, and L-glutamine 2 mM in a humid atmosphere at 37° C and with 5% pCO_2. Cells were passed (using trypsin 0.25%) twice a week when the confluence level was estimated at about 70–90% of the available culture space.

2.13. Proliferation Assay. Membranes were shaped in disks (diameter, 6 mm) and placed, after UV sterilization, in 96-well plates for cell suspension cultures. On each disk, 3000 cells were seeded, adding 200 μL of complete DMEM. Samples were incubated in a humid atmosphere at 37 °C and with 5% pCO_2. Adhesion and proliferation were tested after 1, 3, 6, and 8 days using a Resazurin Cell Viability Assay Kit (Biotium, Fremont, CA, USA) and scanning electron microscopy (SEM) imaging. For the Resazurin assay, eight samples for each type of membrane were tested (two samples were left without cells as blanks). At each time point, the culture medium was removed and 200 μL of Resazurin solution 10% in DMEM was added to the wells. After 4 h of incubation, 150 μL of the solution was taken from each well for fluorescence reading; each well was washed with PBS, and 200 μL of the new medium was added. Fluorescence reading was performed using the spectrofluorometer GloMax Multi+ Detection System (Promega, Madison, WI, USA) under an excitation wavelength of 525 nm and collecting the fluorescence emission in the range 580–640 nm.

For SEM analysis, cells were seeded and cultured on two disks, as described above, for each time point. Membranes were fixed and dehydrated at room temperature. Membranes were washed in PBS and fixed for 45 min with 4% formaldehyde in PBS. Samples were then dehydrated by a stepwise treatment of 30 min with ethanol in water (30, 50, 70, 90, and 100% v/v) and then with hexamethyldisilazane in ethanol (30, 50, 70, 90, and 100% v/v). After 1 h in 100% hexamethyldisilazane, samples were air-dried, sputter-coated with gold (Sputter Coater K550X, Emitech, Quorum Technologies Ltd, UK), and visualized by a scanning electron microscope (Quanta 250 SEM, FEI, Oregon, USA) operated in the secondary electron detection mode. The working distance was adjusted in order to obtain the suitable magnification; the accelerating voltage was set to 30 kV.

2.14. Cytotoxicity Assay. Cell toxicity was tested by measuring the lactate dehydrogenase (LDH) released from MG63 cells cultured in the presence of the membranes using the Lactate Dehydrogenase Activity Colorimetric Assay Kit (BioVision, Milpitas, CA, USA). MG63 was seeded in 24-well plates (30,000 cells per well) and incubated in a humid atmosphere at 37 °C and with 5% pCO_2. After 24 h of incubation, treatment compounds were added to the wells: membranes, polystyrene disks (PS, as a negative surface toxicity control), zinc-embedded polyurethane disks (PU/Zn, as a positive surface toxicity control), and Triton X-100 0.01% (v/v) in PBS (as a positive solution toxicity control). After 24 and 72 h of incubation with the treatment compounds, the medium was collected, and the test was performed following the manufacturer's protocol. The absorbance was measured at 450 nm with the spectrofluorometer GloMax Multi+ Detection System (Promega, Madison, WI, USA) and was corrected with the absorbance of the medium. The percentage cytotoxicity was calculated by dividing the absorbance of the control or treated cells with the absorbance of the reference control cell lysate at 24 and 72 h. Cells were also visualized by optical microscopy after 72 h of treatment in order to evaluate their morphology and density.

2.15. Biofilm Deposition Inhibition Assay. The efficacy of PCL membranes containing CTL-nAg in discouraging the biofilm deposition by of *Pseudomonas aeruginosa* ATCC 27853 and *Staphylococcus aureus* ATCC 25923 was assessed using the tetrazolium salt assay [3-(4,5-dimethylthiazol-2-yl)-2,5-diphenyltetrazolium bromide (MTT test)] to assess biofilm viability and deduce its amount, slightly modifying the protocol reported in the previous work by Mardirossian *et al.*[59]

Bacteria of each species were swiped on LB agar plates from a glycerol stock stored at −80 °C and then incubated overnight at 37 °C. For liquid culture, few bacterial colonies were re-suspended in 4 mL of LB broth and incubated overnight at 37 °C under agitation (140 rpm). The following day, a re-inoculum was performed by diluting an aliquot of both the overnight cultures, 200 μL for *S. aureus* and 400 μL for *P. aeruginosa*, respectively, in 10 mL of new LB broth. The culture was grown for about 90 min at 37 °C under agitation (140 rpm) to an optical density at 600 nm (OD600) $\approx$ 0.3. To estimate the bacterial concentration, predictive models were used, knowing that OD600 = 0.3 indicates a bacterial concentration of 10^7 CFU/mL for *P. aeruginosa* ATCC 27853 and that OD600 = 0.1 indicates a bacterial concentration of 5×10^7 CFU/mL for *S. aureus* ATCC 25923. Bacteria were then diluted to a final concentration of 10^6 CFU/mL in LB 10% (v/v) medium diluted in PBS. 200 μL of diluted bacterial suspension was deposited on the membranes. Some samples were covered with diluted LB only as a control. Samples were incubated for 72 h at 37 °C in a humid atmosphere. At the end of incubation, the exhausted LB medium was removed. To get rid of any sedimented planktonic cells, membranes were washed twice with 300 μL of fresh 10% LB, avoiding disturbing the biofilm with the flow and tipping. Then, each membrane was covered in the dark with 200 μL of 10% LB containing a final concentration of 1 mg/mL of MTT (thiazolyl blue tetrazolium nromide, Sigma-Aldrich); the plate was then sealed with Parafilm to reduce evaporation and covered with aluminum foil and incubated for 4 h at 37 °C in the dark. After incubation, the medium with MTT was removed, and the membranes were washed with 300 μL of PBS. Membranes were then covered with 200 μL of a lysis solution containing 20% (w/v) sodium dodecyl sulfate (Fluka) solved in 50% (v/v) DMF (Romil) in distilled water. The plate was again sealed with Parafilm and aluminum and incubated at 37 °C overnight in the dark. Subsequently, 100 μL of the supernatant was transferred from each sample to a flat-bottom 96-well microtiter plate. Then, the absorbance at 570 nm (A570) was measured with the NanoQuant infinite instrument M200pro (Tecan, Männedorf, Switzerland). Biofilm viability was then calculated as a function of A570.

2.16. Bacterial Viability Assay. Bacterial suspensions of *P. aeruginosa* ATCC 27853 and *S. aureus* ATCC 25923 were prepared as described above to a final concentration of 10^6 CFU/mL in 10% LB in PBS. 120 μL of bacterial suspensions was then incubated in the presence of membrane samples for 60 min at 37 °C under agitation (140 rpm). Before and after the incubation, bacteria underwent serial

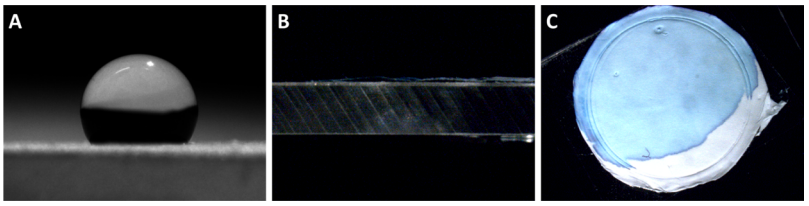

Figure 2. Contact angle analysis of untreated PCL membranes (A) and air−plasma-treated PCL membranes (B). Top view of the air−plasma-treated PCL membrane (C). In this latter image, the blue hue is related to the use of methylene blue as a marker for the diffusion of the liquid phase in the membrane.

Table 1. Contact Angle Values and Surface Energy Values for PCL Membranes Untreated or Treated with the Air−Plasma Treatment

PCL membranes	deionized water contact angle (deg)	diiodomethane contact angle (deg)	γ_s (mJ/m^2)	γ_s^d (mJ/m^2)	γ_s^p (mJ/m^2)
untreated	128 ± 5.7	∼0	58.5 ± 0.1	50.8 ± 0.1	7.7 ± 2.2
air−plasma-treated	∼0	∼0	81.4 ± 0.1	50.8 ± 0.1	30.6 ± 0.1

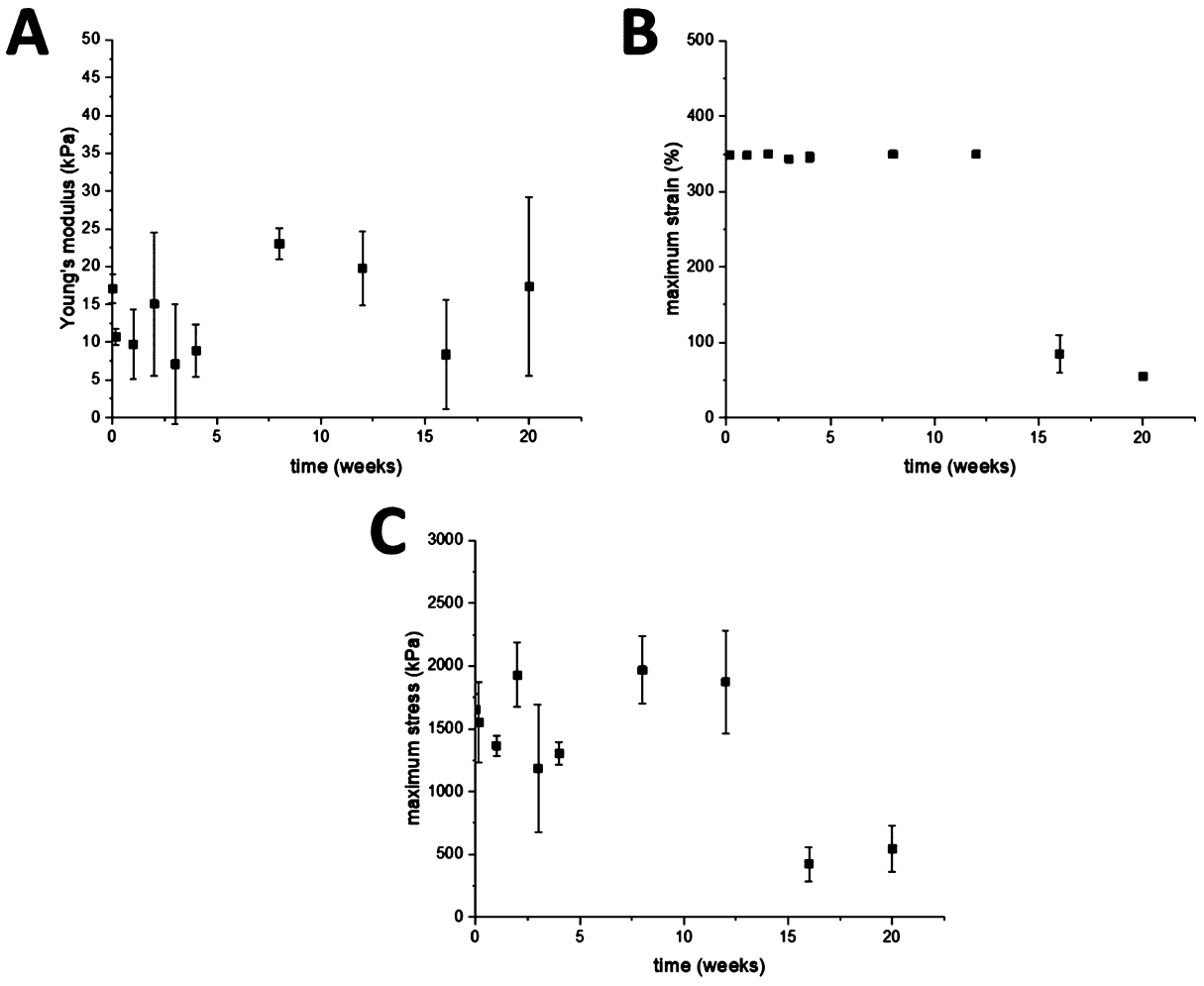

Figure 3. Stability of plasma-treated PCL membranes evaluated as the variation over time of Young's modulus (A), maximum strain (B), and maximum stress (C) reached up to the maximum displacement of DMA or up to sample break.

10-fold dilutions in 10% LB in PBS; then, 50 μL of each dilution was spread on LB−agar plates. The plates were incubated overnight at 37 °C, and the following day, the bacterial colonies growing on the plates were counted to assess any bactericidal effect performed by the membranes during the incubation.

2.17. Statistical Analysis. Statistical analyses were performed by means of Origin software (OriginLab Corporation). Data that satisfied both the normality (Kolmogorov−Smirnov test) and equality variance (Levene's test) assumptions were analyzed with the one-way ANOVA test, applying Bonferroni's correction. Data that did not satisfy normality and equality of variance were analyzed by Kruskal−Wallis and Mann−Whitney U non-parametric tests. The statistical significance was pre-set at $\alpha = 0.05$.

3. RESULTS

3.1. PCL Membrane Preparation and Characterization of the Morphology and Wettability. Electrospun

PCL membranes were prepared by adapting the protocols previously published by Nhi *et al.* and Du *et al.*[15,18] Membranes obtained after 1 h of ELS and subsequently treated for CTL adsorption are reported in Figure 1. Pristine membranes shown in Figure 1A,B clearly show that the air−plasma treatment, performed to increase membrane hydrophilicity, does not alter the fiber morphology and diameter. Moreover, the fiber morphology of air−plasma-treated membranes, after being aged in deionized water for 1 week, remained unaltered (Figure 1C). The diameter of the nanofibers of the pristine membranes is 770 ± 170 nm (Figure 1A); no significant variations ($p > 0.05$) are detected if compared with that of the treated membranes (Figure 1B) or with that of the aged ones (Figure 1C). Membrane thickness is affected by an intrinsic variability of the process and of fiber deposition; the thickness of the membranes varies from about 100 to 300 μm. These values were measured with a caliper by carefully clamping the membranes between two plain microscopy slides.

The protocol for air−plasma treatment was chosen after literature analysis, and its effects were evaluated by contact angle measurements, which revealed the hydrophobicity of untreated membranes (average contact angle, 128 ± 4°, Figure 2A, Table 1) and the high hydrophilicity of treated membranes (contact angles tend to 0°, Figure 2B). Figure 2C reports the top view of the air−plasma-treated membrane reported in Figure 2B; the diffusion of water labeled with methylene blue can be appreciated, indicating the high wettability of these membranes.

Contact angle values and surface energy values, calculated with the Owens−Wendt method,[55] are reported in Table 1. The hydrophobic nature of the untreated PCL membrane can be appreciated by observing the high values of the water contact angle and the low value of the polar component of the surface energy. The effect of air−plasma treatment is an increase of the polar groups on the membrane surface, as can be seen from the increase in the value of the surface energy polar component.

3.2. Characterization of Membrane Stability and Mechanical Properties. Uniaxial tensile tests were performed to characterize the membrane's mechanical properties. Dog bone-shaped membranes were incubated for different time intervals in SBF at 37 °C. Due to the displacement limit of DMA used, it was possible to test the membranes up to 350% of deformation. The elastic modulus variations are shown in Figure 3A; this parameter was almost constant over time, despite the variability associated with the preparation procedure. The maximum deformation (strain) that the membranes can sustain is represented in Figure 3B. Up to 12 weeks, membranes were able to sustain the maximum deformation applicable with the testing machine, that is, 350%. At 16 weeks, some samples broke at 70% strain, and at 20 weeks, some samples broke at 50% strain; for the sake of clarity, data of maximum strain and maximum stress were computed considering only the samples which had undergone complete rupture. The maximum stress trend over time (Figure 3C) is similar to the variation displayed by the elastic modulus, with the variability, around an average value of 1.5 MPa, which in the first 12 weeks can be ascribed to membrane preparation. At 16 and 20 weeks, the membrane rupture indicates a significant decrease of the maximum stress sustainable by the membranes, which is around 500 kPa.

The effects of incubation in SBF are appreciable in Figure 4, in which membranes after 1 day of incubation in SBF (Figure 4A) are compared with the membranes aged for 20 weeks (Figure 4B). From the SEM images (Figure 4), it is possible to appreciate the effects of the longest incubation (20 weeks) on the morphology of the nanofibers, which looked swollen and, in a few cases, broken. These alterations lead to an earlier failure of these membranes (*i.e.*, lower maximum strain and stress, Figure 3B,C) but not to the variation of their elastic modulus (Figure 4A).

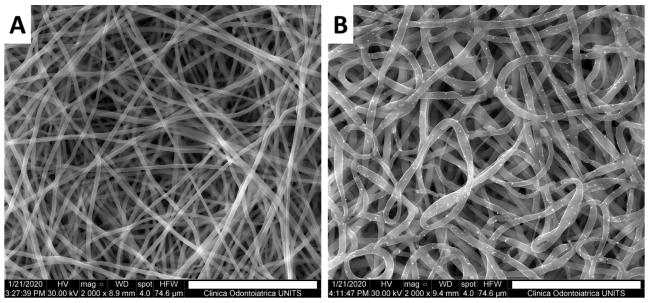

Figure 4. Morphological aspect of membranes soaked in SBF for 1 day (A) and for 20 weeks (B). Swollen and broken nanofibers can be appreciated after 20 weeks of incubation. The scale bar is 30 μm.

3.3. CLT and CTL-nAg Adsorption on PCL Membranes and Characterization of Coating Stability and Silver Release. In order to promote bioactivity, PCL membranes were functionalized by the adsorption of CTL after the air−plasma treatment. The adsorption was performed by soaking the treated membranes in a CTL solution. The effect of air−plasma treatment on the adsorption of CTL is reported in Figure 5. Here, the adsorption of CTL-FITC on untreated membranes (Figure 5A) is compared with the one of the treated membranes (Figure 5B). Confocal laser scanning microscopy revealed that the adsorption process on treated membranes leads to a more uniform and intense fluorescence

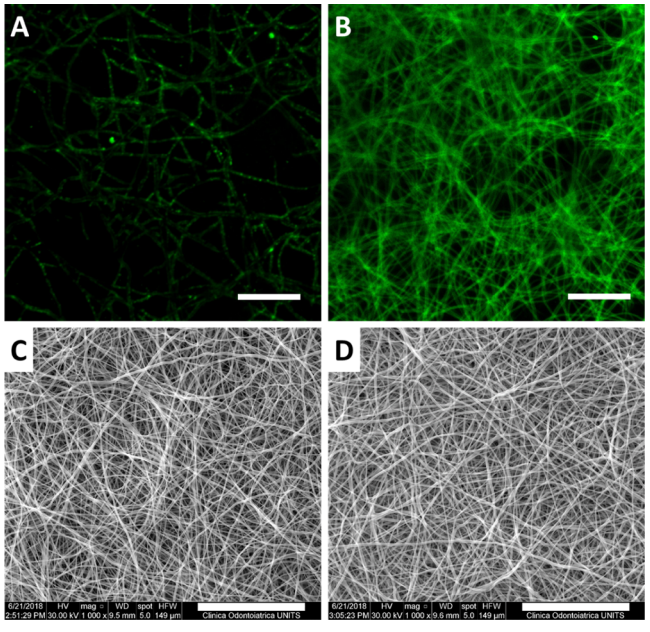

Figure 5. Confocal microscopy images of CTL-FITC adsorbed on untreated PCL membranes (A) and on air−plasma-treated PCL membranes (B). The scale bar is 50 μm. SEM micrographs of PCL membranes (C) and PCL membranes after CTL adsorption (D). Both (C,D) images are related to air−plasma-treated membranes.

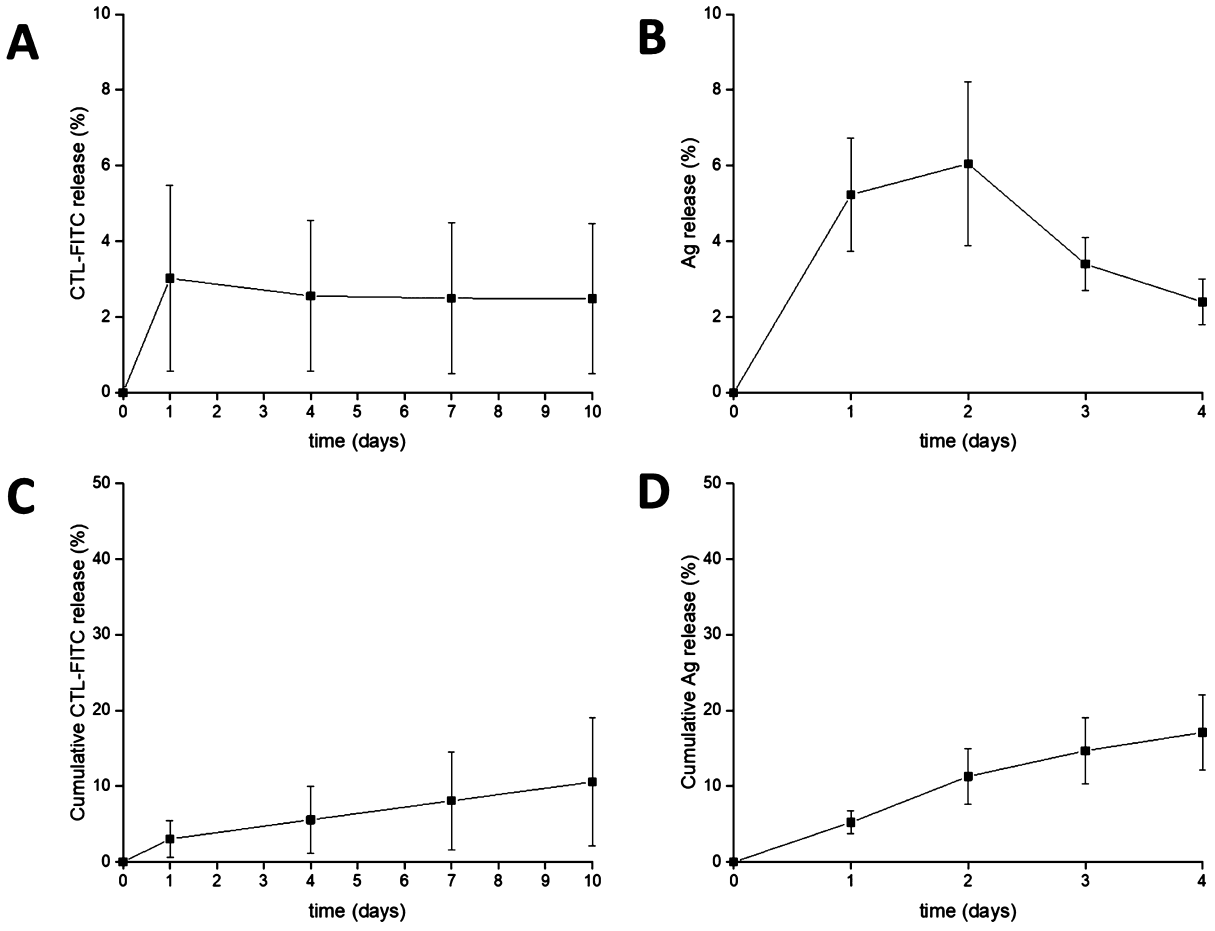

Figure 6. CTL-FITC release from CTL-FITC-coated PCL membranes (A) and silver release from CTL-nAg-coated PCL membranes (B). Cumulative CTL-FITC and silver releases are reported in (C,D), respectively. The released values are calculated as a percentage of the total amount of CTL-FITC and CTL-nAg adsorbed on PCL membranes.

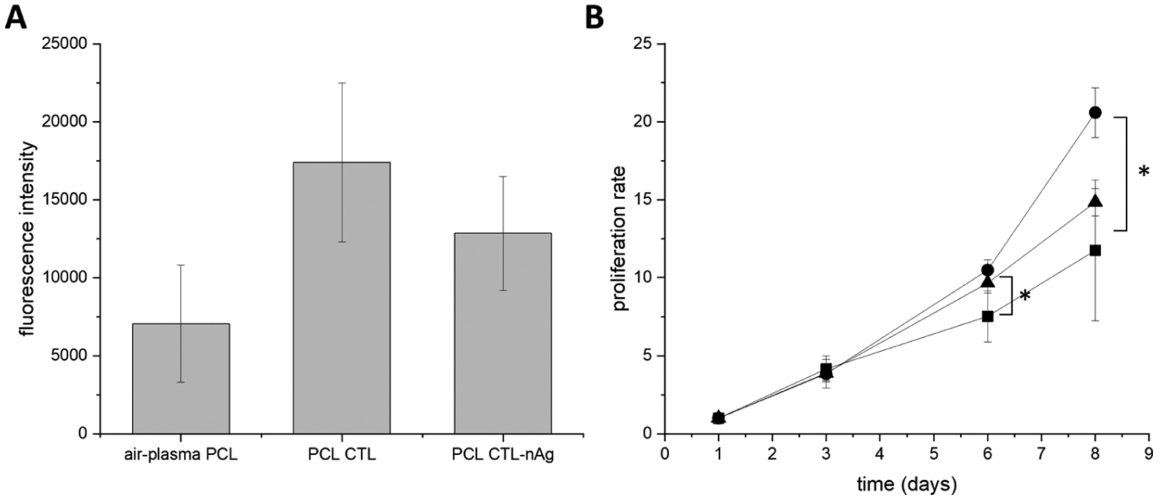

Figure 7. Cell adhesion of MG63 cells expressed as Resazurin fluorescence intensity (A). Proliferation rate of MG63 cells (B) cultured on air–plasma-treated PCL membranes—control (■), coated with CTL (●) or CTL-nAg (▲). Statistically significant differences are indicated with an asterisk (*).

signal with respect to that of the untreated ones, indicating a higher and more homogeneous adsorption of CTL-FITC. Morphological SEM analysis of fibers after CTL adsorption is reported in Figure 5C for untreated membranes and in Figure 5D for air–plasma-treated membranes. Comparing the images with those reported in Figure 1, it can be appreciated that in both cases, CTL adsorption does not alter the fiber morphology, nor is any aggregate of the polymer present.

The stability of CTL or CTL-nAg coatings was assessed by soaking the coated membranes in a saline solution and evaluating the release of CTL-FITC and silver through spectrofluorometric analysis and ICP–MS, respectively. The

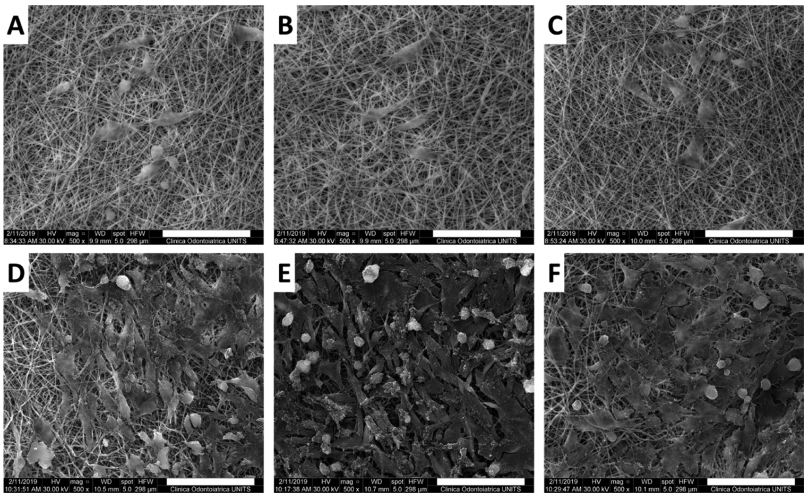

Figure 8. SEM micrographs of MG63 cells seeded on air−plasma-treated bare PCL membranes [(A) day 1; (D) day 8], PCL membranes coated with CTL [(B) day 1; (E) day 8], and PCL membranes coated with CTL-nAg [(C) day 1; (F) day 8]. The scale bar is 100 μm.

analysis of CTL-FITC release, reported in Figure 6A,C, revealed a constant release of CTL-FITC and that after 10 days of incubation, only 10% of the total amount of CTL-FITC adsorbed on the membranes was released, with a linear trend over time. Compared with the release of CTL-FITC, the release of silver (reported in Figure 6B,D) was more rapid; indeed, after only 4 days, 20% of the total amount of silver contained in CTL-nAg-coated PCL membranes was released; moreover, a burst release could be observed at day 1.

3.4. Biological Properties of CTL- and CTL-nAg-Coated PCL Membranes. The ability of membranes to sustain cell adhesion and proliferation was assessed using MG63 cells and the Resazurin assay. Cells were seeded on treated membranes coated with CTL or with CTL-nAg. Uncoated PCL membranes treated with air−plasma treatment were used as a control. Cell adhesion is reported as the intensity of the Resazurin fluorescence signal, after 1 day of cells seeding on the membranes. The data, reported in Figure 7A, show that cell adhesion was significantly higher on CTL-coated membranes with respect to that of air−plasma-treated membranes. In the presence of nAg, the adhesion was slightly lower with respect to that of CTL-coated membranes, but the differences were not statistically significant. The proliferation rate of MG63 cells seeded on modified PCL membranes in Figure 7B shows that the three types of membranes were able to sustain cell adhesion and proliferation on their surface, but in the presence of CTL, a statistically significant increase of cell proliferation could be observed with respect to that of control membranes. PCL membranes coated with CTL-nAg display an intermediate behavior, which was not different from that of control membranes or CTL-coated membranes.

The morphology of MG63 cells seeded on PCL membranes was evaluated with SEM imaging. Cells were seeded on the three types of membrane used for the evaluation of the proliferation rate and were cultured for 1 and 8 days. SEM images of fixed and dehydrated samples are reported in Figure 8: qualitatively, there were no differences in the adhesion, in the spreading, and in the morphology of cells after 1 day of culture on air−plasma-treated membranes (Figure 8A) and on membranes treated with CTL (Figure 8B) and CTL-nAg (Figure 8C). Moreover, after 8 days of culture, there was a uniform layer of cells on all the surfaces.

Cytotoxicity was evaluated to test the effects of nAg and the possible presence of organic solvent residues. MG63 cells were cultured in the presence of the three types of membranes (not coated, coated with CTL, and coated with CTL-nAg), and the toxicity was evaluated as a percentage of released LDH over the total enzymes contained in the cultured cells. Results (reported in Figure 9) were compared with cells treated with

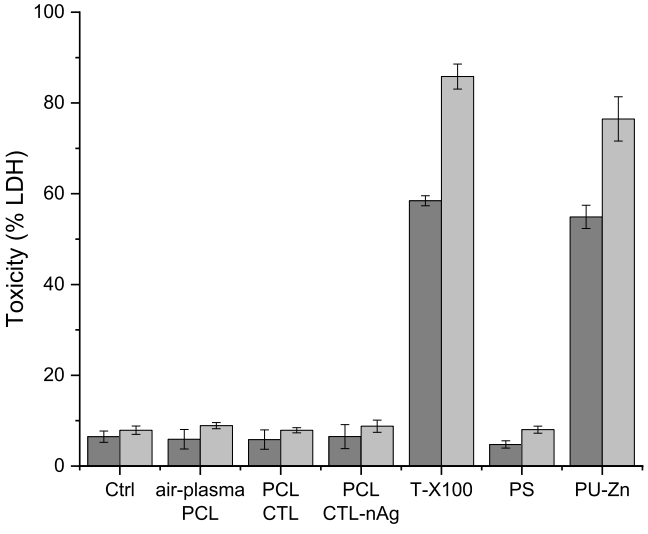

Figure 9. Percentage of LDH released by MG63 cells cultured alone (Ctrl) or in the presence of air−plasma-treated bare PCL membranes (air plasma PCL), PCL coated with CTL (PCL CTL), or PCL coated with CTL-nAg (PCL CTL-nAg). PS is added as a negative control of toxicity; zinc-embedded PU membranes (PU/Zn) and Triton X-100 in PBS (0.01% v/v) are used as positive controls of toxicity. LDH release is reported after 24 h (dark gray) and 72 h (light gray) of treatment.

negative (PS membranes) and positive (Triton X100 and zinc-embedded PU membranes) controls for toxicity. The amount of released LDH from cells treated with the three types of membranes was comparable with those of control cells and cells treated with the negative control for toxicity. The slight increase in toxicity over time is statistically significant only for cells treated with CTL-nAg-coated membranes, but the

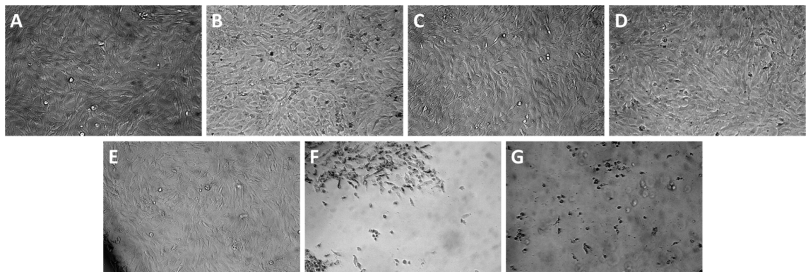

Figure 10. Optical microscopy images of MG63 cells cultured alone (A) or in the presence of air−plasma-treated bare PCL membranes (B), PCL membranes coated with CTL (C), or PCL membranes coated with CTL-nAg (D). PS (E) is added as a negative control of toxicity; zinc-embedded PU membranes (F) and Triton X-100 in PBS (G) are used as positive controls of toxicity.

released LDH values are not different if compared with the negative control values.

The morphology of cells cultured in the presence of membranes and of negative and positive controls for toxicity, used for the LDH assay, was investigated with optical microscopy. Images are reported in Figure 10 and show that MG63 cells cultured in the presence of air−plasma-treated PCL membranes (B) or membranes coated with CTL (C) or CTL-nAg (D) display a cell density and morphology comparable with that of control cells (A) and with that of cells treated with PS membranes (E). On the contrary, cells treated with zinc-embedded PU membranes (F) and Triton X-100 in PBS (G) appear less dense and round-shaped, indicating cell suffering and death.

3.5. Antibacterial Properties of CTL-nAg-Coated PCL Membranes. The potential of CTL-nAg-coated PCL membranes to prevent biofilm formation was evaluated toward reference strains of *P. aeruginosa* and *S. aureus* using the MTT assay. Bacteria were cultured directly on the surface of untreated PCL membranes, air−plasma-treated PCL membranes, and membranes coated with CTL or CTL-nAg. Bacteria were able to form a viable biofilm, in a comparable way, on membranes that do not contain nAgs (Figure 11). On the contrary, biofilm formation on CTL-nAg-coated membranes was strongly inhibited. This effect was more pronounced for *S. aureus*.

The decrease in biofilm deposition could have been due to a surface effect discouraging bacterial adhesion or due to the release of silver ions affecting the bacterial viability. In order to investigate the mechanism of inhibition of biofilm formation, bacteria were also cultured in a suspension with CTL- and CTL-nAg-coated membranes, and their viability was tested with the colony forming unit assay. The silver contained in CTL-nAg-coated membranes did not significantly affect the viability of the bacterial inoculum (Figure 12), suggesting that the inhibition of biofilm formation was due to a surface effect.

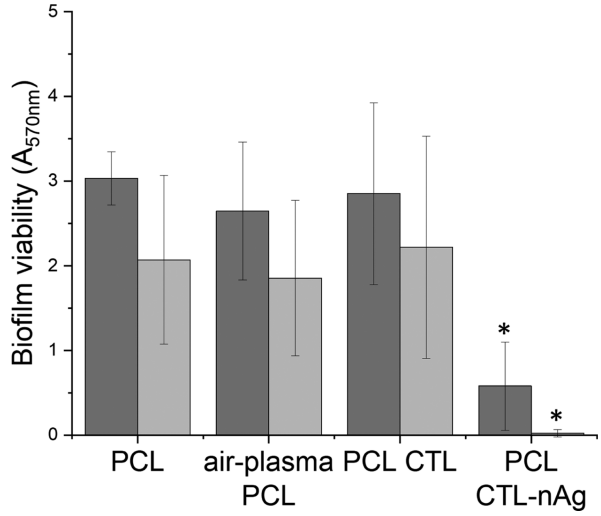

Figure 11. Biofilm viability expressed as absorbance at 570 nm for *P. aeruginosa* ATCC 27853 (dark gray) and *S. aureus* ATCC 25923 (light gray), cultured on untreated PCL membranes (PCL), air−plasma-treated bare PCL membranes (air-plasma PCL), or PCL membranes coated with CTL (PCL CTL) or CTL-nAg (PCL CTL-nAg).

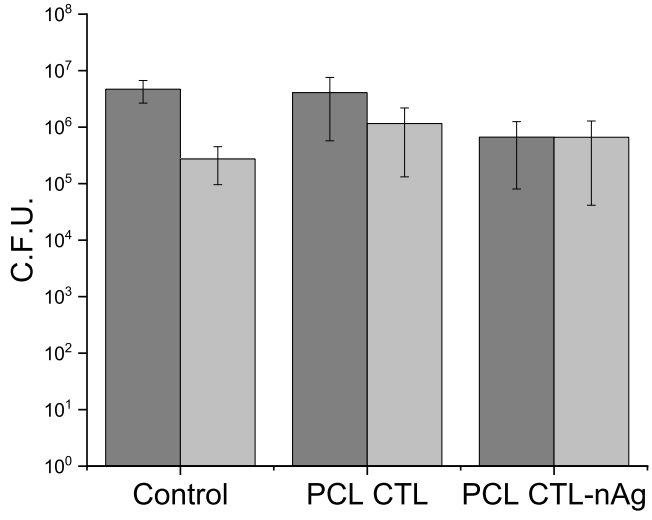

Figure 12. Viability of *P. aeruginosa* ATCC 27853 (dark gray) and *S. aureus* ATCC 25923 (light gray) exposed for 60 min to plasma-treated PCL membranes coated with CTL (PCL CTL) and CTL-nAg (PCL CTL-nAg).

4. DISCUSSION

This work describes a strategy for the preparation of electrospun membranes implemented with bioactive and antibacterial properties. PCL was chosen because of its proven suitability for the preparation of biomaterials like scaffolds, 3D printed constructs, and nanofiber-based membranes.[4,5,11] The protocol adopted here was inspired by the studies of Nhi *et al.* and Du *et al.*[15,18] The parameters of the ELS process (polymer concentration, solvent mixture composition, voltage, flow rate, needle diameter, and needle-to-target distance) were tuned and selected in order to optimize the process (*e.g.*, avoiding the obstruction of the needle and ensuring the stability of Taylor's cone) and to obtain stable and handleable membranes with a homogeneous distribution of nanofibers and without macro-

scopic and microscopic defects. The membrane's stability in SBF was assessed up to 20 weeks. The membranes proved to be able to maintain their mechanical properties unaltered up to 12 weeks, with values of the elastic modulus, tensile strength, and deformation at break being similar to those reported for this type of membrane.[2,5,60] The variability of the data, which can be appreciated by observing the standard deviations, in particular for Young's modulus, can be ascribed to the ELS process and to the preparation of membranes and samples. After 12 weeks, the decay of resistance was evident for some membranes, but they were still able to sustain deformations that allow them to be considered suitable for GBR and GTR applications.[61]

Despite its stability and mechanical properties, hydrophobicity of PCL hampers its use in biological applications. To overcome this issue, air−plasma treatment was used to increase membrane hydrophilicity. This treatment protocol was chosen because of its already proven effects on PCL and on other substrates like polydimethylsiloxane scaffolds;[19,23] the increase of hydrophilicity was confirmed by both contact angle measurements and surface energy analysis. In particular, the application of the Owens−Wendt method, which was optimized for the analysis of polymer surface energy,[55] allowed us to calculate the surface energy and to confirm that the increase of hydrophilicity and wettability can be ascribed to the increase of the polar groups on the air−plasma-treated membrane surface. This effect was already observed by Can-Herrera *et al.* for PCL membranes treated for 5 min with air−plasma at the power of 10 W.[21] Despite the effects of the air−plasma treatment in terms of surface wettability and surface energy variation, the analyses performed with ATR−FTIR, XPS, and NEXAFS spectroscopies (data not showed) did not reveal any differences in the chemical composition or in the concentration of oxygen and nitrogen elements between untreated and air−plasma-treated membranes. On the contrary, it was demonstrated that the effects of air−plasma treatment on PCL nanofiber-based membranes are an increase in oxygen and nitrogen concentrations and the formation of carboxylic groups.[21] It is possible that, in the case reported in this work, the applied power and treatment time of the air−plasma treatment process are not sufficient to appreciate the variation of the elemental composition with the techniques adopted here. This hypothesis could be supported by the fact that, in contrast to what was observed by Can-Herrera *et al.*,[21] after the air−plasma treatment, there is no variation of the diiodomethane contact angle and of the dispersive component of surface energy.

The chemical modification introduced by the air−plasma treatment was preparatory to the chemical adsorption of CTL. As already observed for methacrylate thermosets,[29] glass slides,[28] and alginate scaffolds,[40] negatively charged surfaces can be covered with a homogeneous coating of CTL, whose positively charged amine groups interact with the carboxylic groups of PCL exposed after the air−plasma treatment.[23,62] One of the most used bioactive compounds to enhance the biological properties of antibacterial PCL membranes is gelatin, which can be included in the PCL nanofibers[5,27,63] or used as a separate layer of electrospun nanofibers to be combined with PCL nanofiber membranes.[26] In this context, the use of CTL as a bioactive coating allows us to use a single step of ELS for the preparation of PCL membranes without the necessity of the preparation of CTL nanofibers and the use of specific conditions for the processing of this highly water-soluble polymer. Then, using CTL as a coating, core−shell-like structured nanofibers can be obtained, with PCL as the core component and CTL as a thin layer, which does not alter the nanofibrous architecture of the membrane. The stability of the coating is of paramount importance to guarantee the presence of CTL in the initial phases of cell adhesion and proliferation; as confirmed by release studies, CTL release from PCL membranes proceeded slowly over time, as already observed for alginate scaffolds coated with CTL.[40] The stability of the CTL coating is important also to guarantee the presence of nAgs and thus the conservation of the antibacterial properties over time. Among the protocols proposed in the literature for nAg preparation and incorporation,[25,47] the one proposed here has the advantage of being easily applied, requiring mild conditions and harmless and nontoxic compounds. Moreover, in a single step, it allows us to obtain a compound, which at the same time can be used to stabilize nAgs and to provide a bioactive and antibacterial coating for biomaterials. Silver can be released from the membrane in the form of nanoparticles when these detach from CTL or when CTL is released, and in the form of ions from the dissolution of nAgs.[45,64,65] The method adopted here for the quantification of released silver does not allow for discrimination between its forms (ions or nanoparticles) and revealed that the released amount of silver, over the total silver contained in membranes, was higher with respect to the amount of CTL released. The release profile is different from those reported previously for other materials prepared with CTL-nAg,[51] probably because of the high surface/volume ratio of electrospun membranes, which increases the active surface, in agreement with the results reported by Nhi *et al.*[18] After the initial burst release of silver, which could provide a strong antibacterial effect in the initial phases of tissue healing, the silver release diminishes, guaranteeing the presence of nAgs on the surface, following a trend similar to that observed for PCL and collagen membranes containing nAgs.[25,47,48] Since the effects of air−plasma treatment in the improvement of cell adhesion have already been tested and proven,[17,18] untreated PCL membranes were not included in these studies; thus, the effects of CTL and CTL-nAg coatings were compared with that of the reference bare air−plasma-treated PCL membranes. The results of cell adhesion and proliferation showed that the presence of CTL and CTL-nAg improved the performances of air−plasma-treated PCL membranes. It can be speculated that the presence of a bioactive coating improves the biological effects of the air−plasma treatment (*i.e.*, hydrophilicity increase) in a different but analogous way with what was observed for neurons grown on glass slides coated with polysaccharides.[28] The proliferation of MG63 cells on CTL- and CTL-nAg-coated membranes confirmed that the CTL coating maintains a biological role despite the polysaccharide release observed over time. The biological tests and SEM micrographs also showed that the presence of nAgs did not hamper the adhesion and the proliferation of MG63 cells; a slight negative effect was observable after 8 days of proliferation, but it could be due to experimental limits, as already observed for *in vitro* evaluations of nAg biological properties.[51,66] Despite a small effect on cell adhesion and proliferation, the presence of silver resulted to be not cytotoxic, as determined by LDH release, which was comparable between cells cultured in the presence of CTL-nAg, control cells, and cells cultured in the presence of CTL-coated membranes and air−plasma-treated membranes.[41,61] In particular, the bio-

compatibility of CTL-nAg membranes in the first day of the experiment proved that the burst release of silver was not harmful for cells. Moreover, the lack of cytotoxic effects of CTL-coated membranes and air−plasma-treated PCL membranes allowed excluding any harmful effect of organic solvent residues.[67]

The MTT assay performed to assess biofilm formation and viability showed that nAgs prevented the biofilm formation in a poor culture medium for *P. aeruginosa* and *S. aureus* on CTL-nAg coated membranes.[41,68] Biofilm formation occurred, for both the bacterial strains tested, in the same way on untreated PCL membranes, air−plasma-treated membranes and CTL-coated membranes; thus, it was independent of the membrane hydrophilicity. Interestingly, for both the bacterial strains tested, the amount of silver released from CTL-nAg-coated membranes was not sufficient to exert a toxic effect on bacterial cells in suspension. Thus, under the tested conditions, nAg activity is mostly an inhibition of bacteria adhesion and biofilm formation on membranes. It is possible that in the case described here, the silver ions were sequestered by ions and proteins in the medium and were not active against bacterial cells.[64] Further studies are necessary to evaluate if the slow release of silver ions is able to exert a long-term antibacterial effect.

The considerations that can be made about the material developed here are limited by two aspects, which regard the *in vitro* and *in vivo* evaluation of biological properties. It will be necessary to evaluate these properties not only in terms of cell adhesion and proliferation but also in terms of differentiation and extracellular matrix deposition on other cell models like human primary cells or mesenchymal stem cells. Moreover, as the *in vivo* environment can affect the stability of the material coating and the release of silver and CTL, these kinds of studies coupled with infection models will be necessary to confirm the bioactive and the antibacterial properties of the material.

5. CONCLUSIONS

Nanofiber-based PCL membranes with bioactive and antibacterial properties were prepared and characterized. Membranes showed excellent stability over time in physiological-like conditions. CTL and CTL-nAg adsorption on membranes resulted in stable coatings, which slowly released CTL and silver over time, guaranteeing the simultaneous presence of both of these components. The biological characterization of the devices investigated here showed an improved adhesion and proliferation of MG63 cells seeded on CTL-coated membranes and the lack of cytotoxic effects of CTL-nAg. Moreover, the CTL-nAg coating could prevent bacterial adhesion and biofilm formation. Overall, the stability and the biological and antimicrobial properties suggest these membranes as a valid tool for the preparation of devices for applications in GBR and GTR and also in other fields such as wound healing and surgical wound dressing.

AUTHOR INFORMATION

Corresponding Author

Davide Porrelli − *Department of Medicine, Surgery and Health Sciences, University of Trieste, 34129 Trieste, Italy;* orcid.org/0000-0002-6437-7646; Phone: +39 040 399 2168; Email: dporrelli@units.it

Authors

Mario Mardirossian − *Department of Medicine, Surgery and Health Sciences, University of Trieste, 34129 Trieste, Italy*

Luigi Musciacchio − *Department of Medicine, Surgery and Health Sciences, University of Trieste, 34129 Trieste, Italy*

Micol Pacor − *Department of Medicine, Surgery and Health Sciences, University of Trieste, 34129 Trieste, Italy*

Federico Berton − *Department of Medicine, Surgery and Health Sciences, University of Trieste, 34129 Trieste, Italy*

Matteo Crosera − *Department of Chemical and Pharmaceutical Sciences, University of Trieste, 34127 Trieste, Italy;* orcid.org/0000-0001-5950-093X

Gianluca Turco − *Department of Medicine, Surgery and Health Sciences, University of Trieste, 34129 Trieste, Italy;* orcid.org/0000-0001-5699-2131

Complete contact information is available at: https://pubs.acs.org/10.1021/acsami.1c01016

Notes

The authors declare the following competing financial interest(s): The author Gianluca Turco declares to be a shares holder of the company BiopoLife.

ACKNOWLEDGMENTS

Financial support was received from the University of Trieste fund program: Finanziamento di Ricerca di Ateneo, FRA 2016, by G.T. for the project entitled "Produzione e caratterizzazione di matrici nanostrutturate a base di bio-polimeri naturali ottenute da electrospinning, applicazioni biomediche di medicina rigenerativa" (code U17-FRATURCO-16). The authors would like to thank Dr. Denis Scaini (SISSA, Trieste, Italy) for his help with air−plasma treatments. The authors would also like to thank Dr. Silvia Nappini and Dr. Elena Magnano (TASC laboratory, IOM, CNR, Basovizza, Trieste, Italy) for their help with XPS and NEXAFS analyses.

REFERENCES

(1) Berton, F.; Porrelli, D.; Di Lenarda, R.; Turco, G. A Critical Review on the Production of Electrospun Nanofibres for Guided Bone Regeneration in Oral Surgery. *Nanomaterials* **2020**, *10*, 16.

(2) Guo, S.; He, L.; Yang, R.; Chen, B.; Xie, X.; Jiang, B.; Weidong, T.; Ding, Y. Enhanced Effects of Electrospun Collagen-Chitosan Nanofiber Membranes on Guided Bone Regeneration. *J. Biomater. Sci., Polym. Ed.* **2020**, *31*, 155−168.

(3) Lian, M.; Sun, B.; Qiao, Z.; Zhao, K.; Zhou, X.; Zhang, Q.; Zou, D.; He, C.; Zhang, X. Bi-Layered Electrospun Nanofibrous Membrane with Osteogenic and Antibacterial Properties for Guided Bone Regeneration. *Colloids Surf., B* **2019**, *176*, 219−229.

(4) Nasajpour, A.; Ansari, S.; Rinoldi, C.; Rad, A. S.; Aghaloo, T.; Shin, S. R.; Mishra, Y. K.; Adelung, R.; Swieszkowski, W.; Annabi, N.; Khademhosseini, A.; Moshaverinia, A.; Tamayol, A. A Multifunctional Polymeric Periodontal Membrane with Osteogenic and Antibacterial Characteristics. *Adv. Funct. Mater.* **2018**, *28*, 1703437.

(5) Shi, R.; Xue, J.; He, M.; Chen, D.; Zhang, L.; Tian, W. Structure, Physical Properties, Biocompatibility and in Vitro/Vivo Degradation Behavior of Anti-Infective Polycaprolactone-Based Electrospun Membranes for Guided Tissue/Bone Regeneration. *Polym. Degrad. Stab.* **2014**, *109*, 293−306.

(6) Lu, S.; Wang, P.; Zhang, F.; Zhou, X.; Zuo, B.; You, X.; Gao, Y.; Liu, H.; Tang, H. A Novel Silk Fibroin Nanofibrous Membrane for Guided Bone Regeneration: A Study in Rat Calvarial Defects. *Am. J. Transl. Res.* **2015**, *7*, 2244−2253.

(7) Liu, J.; Kerns, D. G. Mechanisms of Guided Bone Regeneration: A Review. *Open Dent. J.* **2014**, *8*, 56−65.

(8) Lotfi, G.; Shokrgozar, M. A.; Mofid, R.; Abbas, F. M.; Ghanavati, F.; Baghban, A. A.; Yavari, S. K.; Pajoumshariati, S. Biological Evaluation (in Vitro and in Vivo) of Bilayered Collagenous Coated (Nano Electrospun and Solid Wall) Chitosan Membrane for Periodontal Guided Bone Regeneration. *Ann. Biomed. Eng.* **2016**, *44*, 2132−2144.
(9) Zafar, M.; Najeeb, S.; Khurshid, Z.; Vazirzadeh, M.; Zohaib, S.; Najeeb, B.; Sefat, F. Potential of Electrospun Nanofibers for Biomedical and Dental Applications. *Materials* **2016**, *9*, 73.
(10) Ren, K.; Wang, Y.; Sun, T.; Yue, W.; Zhang, H. Electrospun PCL/Gelatin Composite Nanofiber Structures for Effective Guided Bone Regeneration Membranes. *Mater. Sci. Eng., C* **2017**, *78*, 324−332.
(11) Xia, Y.; Yao, J.; Li, N.; Shao, C.-H.; Shen, X.-Y.; Xie, L.-Z.; Chen, G.; Zhang, F.-M.; Gu, N. Electrospun Poly(Butylene Carbonate) Membranes for Guided Bone Regeneration: In Vitro and in Vivo Studies. *J. Bioact. Compat. Polym.* **2014**, *29*, 486−499.
(12) Savelyeva, M. S.; Abalymov, A. A.; Lyubun, G. P.; Vidyasheva, I. V.; Yashchenok, A. M.; Douglas, T. E. L.; Gorin, D. A.; Parakhonskiy, B. V. Vaterite Coatings on Electrospun Polymeric Fibers for Biomedical Applications. *J. Biomed. Mater. Res., Part A* **2017**, *105*, 94−103.
(13) Tortora, L.; Concolato, S.; Urbini, M.; Giannitelli, S. M.; Basoli, F.; Rainer, A.; Trombetta, M.; Orsini, M.; Mozetic, P. Functionalization of Poly(e-Caprolactone) Surface with Lactose-Modified Chitosan via Alkaline Hydrolysis: ToF-SIMS Characterization. *Biointerphases* **2016**, *11*, 02A323.
(14) Santocildes-Romero, M. E.; Goodchild, R. L.; Hatton, P. V.; Crawford, A.; Reaney, I. M.; Miller, C. A. Preparation of Composite Electrospun Membranes Containing Strontium-Substituted Bioactive Glasses for Bone Tissue Regeneration. *Macromol. Mater. Eng.* **2016**, *301*, 972−981.
(15) Du, L.; Xu, H.; Zhang, Y.; Zou, F. Electrospinning of Polycaprolatone Nanofibers with DMF Additive: The Effect of Solution Proprieties on Jet Perturbation and Fiber Morphologies. *Fibers Polym.* **2016**, *17*, 751−759.
(16) Azimi, B.; Nourpanah, P.; Rabiee, M.; Arbab, S. Poly (ϵ-caprolactone) Fiber: An Overview. *J. Eng. Fibers Fabr.* **2014**, *9*, 155892501400900309.
(17) Aldemir Dikici, B.; Dikici, S.; Reilly, G. C.; MacNeil, S.; Claeyssens, F. A Novel Bilayer Polycaprolactone Membrane for Guided Bone Regeneration: Combining Electrospinning and Emulsion Templating. *Materials* **2019**, *12*, 2643.
(18) Nhi, T. T.; Khon, H. C.; Hoai, N. T. T.; Bao, B. C.; Quyen, T. N.; Van Toi, V.; Hiep, N. T. Fabrication of Electrospun Polycaprolactone Coated Withchitosan-Silver Nanoparticles Membranes for Wound Dressing Applications. *J. Mater. Sci.: Mater. Med.* **2016**, *27*, 156.
(19) Bosi, S.; Rauti, R.; Laishram, J.; Turco, A.; Lonardoni, D.; Nieus, T.; Prato, M.; Scaini, D.; Ballerini, L. From 2D to 3D: Novel Nanostructured Scaffolds to Investigate Signalling in Reconstructed Neuronal Networks. *Sci. Rep.* **2015**, *5*, 9562.
(20) Wiącek, A. E.; Terpiłowski, K.; Jurak, M.; Worzakowska, M. Low-Temperature Air Plasma Modification of Chitosan-Coated PEEK Biomaterials. *Polym. Test.* **2016**, *50*, 325−334.
(21) Can-Herrera, L. A.; Ávila-Ortega, A.; de la Rosa-García, S.; Oliva, A. I.; Cauich-Rodríguez, J. V.; Cervantes-Uc, J. M. Surface Modification of Electrospun Polycaprolactone Microfibers by Air Plasma Treatment: Effect of Plasma Power and Treatment Time. *Eur. Polym. J.* **2016**, *84*, 502−513.
(22) Rymuszka, D.; Terpiłowski, K.; Borowski, P.; Holysz, L. Time-Dependent Changes of Surface Properties of Polyether Ether Ketone Caused by Air Plasma Treatment. *Polym. Int.* **2016**, *65*, 827−834.
(23) Hosseini, F. S.; Enderami, S. E.; Hadian, A.; Abazari, M. F.; Ardeshirylajimi, A.; Saburi, E.; Soleimanifar, F.; Nazemisalman, B. Efficient Osteogenic Differentiation of the Dental Pulp Stem Cells on β-Glycerophosphate Loaded Polycaprolactone/Polyethylene Oxide Blend Nanofibers. *J. Cell. Physiol.* **2019**, *234*, 13951−13958.
(24) Cirillo, V.; Guarino, V.; Ambrosio, L. Design of Bioactive Electrospun Scaffolds for Bone Tissue Engineering. *J. Appl. Biomater. Funct. Mater.* **2012**, *10*, 223−228.
(25) Abdelaziz, D.; Hefnawy, A.; Al-Wakeel, E.; El-Fallal, A.; El-Sherbiny, I. M. New Biodegradable Nanoparticles-in-Nanofibers Based Membranes for Guided Periodontal Tissue and Bone Regeneration with Enhanced Antibacterial Activity. *J. Adv. Res.* **2021**, *28*, 51−62.
(26) He, M.; Wang, Q.; Xie, L.; Wu, H.; Zhao, W.; Tian, W. Hierarchically Multi-Functionalized Graded Membrane with Enhanced Bone Regeneration and Self-Defensive Antibacterial Characteristics for Guided Bone Regeneration. *Chem. Eng. J.* **2020**, *398*, 125542.
(27) Xue, J.; Shi, R.; Niu, Y.; Gong, M.; Coates, P.; Crawford, A.; Chen, D.; Tian, W.; Zhang, L. Fabrication of Drug-Loaded Anti-Infective Guided Tissue Regeneration Membrane with Adjustable Biodegradation Property. *Colloids Surf., B* **2015**, *135*, 846−854.
(28) Medelin, M.; Porrelli, D.; Aurand, E. R.; Scaini, D.; Travan, A.; Borgogna, M. A.; Cok, M.; Donati, I.; Marsich, E.; Scopa, C.; Scardigli, R.; Paoletti, S.; Ballerini, L. Exploiting Natural Polysaccharides to Enhance in Vitro Bio-Constructs of Primary Neurons and Progenitor Cells. *Acta Biomater.* **2018**, *73*, 285−301.
(29) Marsich, E.; Travan, A.; Donati, I.; Turco, G.; Kulkova, J.; Moritz, N.; Aro, H. T.; Crosera, M.; Paoletti, S. Biological Responses of Silver-Coated Thermosets: An in Vitro and in Vivo Study. *Acta Biomater.* **2013**, *9*, 5088−5099.
(30) Scognamiglio, F.; Travan, A.; Donati, I.; Borgogna, M.; Marsich, E. A Hydrogel System Based on a Lactose-Modified Chitosan for Viscosupplementation in Osteoarthritis. *Carbohydr. Polym.* **2020**, *248*, 116787.
(31) Donati, I.; Feresini, M.; Travan, A.; Marsich, E.; Lapasin, R.; Paoletti, S. Polysaccharide-Based Polyanion-Polycation-Polyanion Ternary Systems. A Preliminary Analysis of Interpolyelectrolyte Interactions in Dilute Solutions. *Biomacromolecules* **2011**, *12*, 4044−4056.
(32) Marsich, E.; Borgogna, M.; Donati, I.; Mozetic, P.; Strand, B. L.; Salvador, S. G.; Vittur, F.; Paoletti, S. Alginate/Lactose-Modified Chitosan Hydrogels: A Bioactive Biomaterial for Chondrocyte Encapsulation. *J. Biomed. Mater. Res., Part A* **2008**, *84A*, 364−376.
(33) Scognamiglio, F.; Travan, A.; Borgogna, M.; Donati, I.; Marsich, E. Development of Biodegradable Membranes for the Delivery of a Bioactive Chitosan-Derivative on Cartilage Defects: A Preliminary Investigation. *J. Biomed. Mater. Res., Part A* **2020**, *108*, 1534−1545.
(34) Tarusha, L.; Paoletti, S.; Travan, A.; Marsich, E. Alginate Membranes Loaded with Hyaluronic Acid and Silver Nanoparticles to Foster Tissue Healing and to Control Bacterial Contamination of Non-Healing Wounds. *J. Mater. Sci.: Mater. Med.* **2018**, *29*, 22.
(35) Vecchies, F.; Sacco, P.; Decleva, E.; Menegazzi, R.; Porrelli, D.; Donati, I.; Turco, G.; Paoletti, S.; Marsich, E. Complex Coacervates between a Lactose-Modified Chitosan and Hyaluronic Acid as Radical-Scavenging Drug Carriers. *Biomacromolecules* **2018**, *19*, 3936−3944.
(36) Liu, Q.; Sacco, P.; Marsich, E.; Furlani, F.; Arib, C.; Djaker, N.; de la Chapelle, M. L.; Donati, I.; Spadavecchia, J. Lactose-Modified Chitosan Gold(III)-PEGylated Complex-Bioconjugates: From Synthesis to Interaction with Targeted Galectin-1 Protein. *Bioconjugate Chem.* **2018**, *29*, 3352−3361.
(37) D'Amelio, N.; Esteban, C.; Coslovi, A.; Feruglio, L.; Uggeri, F.; Villegas, M.; Benegas, J.; Paoletti, S.; Donati, I. Insight into the Molecular Properties of Chitlac, a Chitosan Derivative for Tissue Engineering. *J. Phys. Chem. B* **2013**, *117*, 13578−13587.
(38) Donati, I.; Stredanska, S.; Silvestrini, G.; Vetere, A.; Marcon, P.; Marsich, E.; Mozetic, P.; Gamini, A.; Paoletti, S.; Vittur, F. The Aggregation of Pig Articular Chondrocyte and Synthesis of Extracellular Matrix by a Lactose-Modified Chitosan. *Biomaterials* **2005**, *26*, 987−998.
(39) Wang, B.; Hu, Q.; Wan, T.; Yang, F.; Cui, L.; Hu, S.; Gong, B.; Li, M.; Zheng, Q. C. Porous Lactose-Modified Chitosan Scaffold for

Liver Tissue Engineering: Influence of Galactose Moieties on Cell Attachment and Mechanical Stability. *Int. J. Polym. Sci.* **2016**, *2016*, 2862738.
(40) Marsich, E.; Bellomo, F.; Turco, G.; Travan, A.; Donati, I.; Paoletti, S. Nano-Composite Scaffolds for Bone Tissue Engineering Containing Silver Nanoparticles: Preparation, Characterization and Biological Properties. *J. Mater. Sci.: Mater. Med.* **2013**, *24*, 1799−1807.
(41) Liu, M.; Luo, G.; Wang, Y.; He, W.; Liu, T.; Zhou, D.; Hu, X.; Xing, M.; Wu, J. Optimization and Integration of Nanosilver on Polycaprolactone Nanofibrous Mesh for Bacterial Inhibition and Wound Healing in Vitro and in Vivo. *Int. J. Nanomed.* **2017**, *12*, 6827−6840.
(42) He, M.; Jiang, H.; Wang, R.; Xie, Y.; Zhao, C. Fabrication of Metronidazole Loaded Poly (ε-Caprolactone)/Zein Core/Shell Nanofiber Membranes via Coaxial Electrospinning for Guided Tissue Regeneration. *J. Colloid Interface Sci.* **2017**, *490*, 270−278.
(43) He, P.; Li, Y.; Huang, Z.; Guo, Z.-Z.; Luo, B.; Zhou, C.-R.; Li, H. A Multifunctional Coaxial Fiber Membrane Loaded with Dual Drugs for Guided Tissue Regeneration. *J. Biomater. Appl.* **2020**, *34*, 1041−1051.
(44) Shi, R.; Ye, J.; Li, W.; Zhang, J.; Li, J.; Wu, C.; Xue, J.; Zhang, L. Infection-Responsive Electrospun Nanofiber Mat for Antibacterial Guided Tissue Regeneration Membrane. *Mater. Sci. Eng., C* **2019**, *100*, 523−534.
(45) Lansdown, A. B. G. A Pharmacological and Toxicological Profile of Silver as an Antimicrobial Agent in Medical Devices. *Adv. Pharmacol. Sci.* **2010**, *2010*, 910686.
(46) Marques, L.; Martinez, G.; Guidelli, É.; Tamashiro, J.; Segato, R.; Payão, S. L. M.; Baffa, O.; Kinoshita, A. Performance on Bone Regeneration of a Silver Nanoparticle Delivery System Based on Natural Rubber Membrane NRL-AgNP. *Coatings* **2020**, *10*, 323.
(47) Chen, P.; Wu, Z.; Leung, A.; Chen, X.; Landao-Bassonga, E.; Gao, J.; Chen, L.; Zheng, M.; Yao, F.; Yang, H.; Lidgren, L.; Allan, B.; Liu, Y.; Wang, T.; Zheng, M. Fabrication of a Silver Nanoparticle-Coated Collagen Membrane with Anti-Bacterial and Anti-Inflammatory Activities for Guided Bone Regeneration. *Biomed. Mater.* **2018**, *13*, 065014.
(48) Qian, Y.; Zhou, X.; Zhang, F.; Diekwisch, T. G. H.; Luan, X.; Yang, J. Triple PLGA/PCL Scaffold Modification Including Silver Impregnation, Collagen Coating, and Electrospinning Significantly Improve Biocompatibility, Antimicrobial, and Osteogenic Properties for Orofacial Tissue Regeneration. *ACS Appl. Mater. Interfaces* **2019**, *11*, 37381−37396.
(49) Wang, J.; Zhan, L.; Zhang, X.; Wu, R.; Liao, L.; Wei, J. Silver Nanoparticles Coated Poly(L-Lactide) Electrospun Membrane for Implant Associated Infections Prevention. *Front. Pharmacol.* **2020**, *11*. DOI: DOI: 10.3389/fphar.2020.00431.
(50) Travan, A.; Pelillo, C.; Donati, I.; Marsich, E.; Benincasa, M.; Scarpa, T.; Semeraro, S.; Turco, G.; Gennaro, R.; Paoletti, S. Non-Cytotoxic Silver Nanoparticle-Polysaccharide Nanocomposites with Antimicrobial Activity. *Biomacromolecules* **2009**, *10*, 1429−1435.
(51) Porrelli, D.; Travan, A.; Turco, G.; Crosera, M.; Borgogna, M.; Donati, I.; Paoletti, S.; Adami, G.; Marsich, E. Antibacterial-Nanocomposite Bone Filler Based on Silver Nanoparticles and Polysaccharides. *J. Tissue Eng. Regener. Med.* **2018**, *12*, e747−e759.
(52) Furlani, F.; Sacco, P.; Marsich, E.; Donati, I.; Paoletti, S. Highly Monodisperse Colloidal Coacervates Based on a Bioactive Lactose-Modified Chitosan: From Synthesis to Characterization. *Carbohydr. Polym.* **2017**, *174*, 360−368.
(53) Schindelin, J.; Arganda-Carreras, I.; Frise, E.; Kaynig, V.; Longair, M.; Pietzsch, T.; Preibisch, S.; Rueden, C.; Saalfeld, S.; Schmid, B.; Tinevez, J.-Y.; White, D. J.; Hartenstein, V.; Eliceiri, K.; Tomancak, P.; Cardona, A. Fiji: An Open-Source Platform for Biological-Image Analysis. *Nat. Methods* **2012**, *9*, 676−682.
(54) Zangrando, M.; Zacchigna, M.; Finazzi, M.; Cocco, D.; Rochow, R.; Parmigiani, F. Polarized High-Brilliance and High-Resolution Soft x-Ray Source at ELETTRA: The Performance of Beamline BACH. *Rev. Sci. Instrum.* **2004**, *75*, 31−36.
(55) Owens, D. K.; Wendt, R. C. Estimation of the Surface Free Energy of Polymers. *J. Appl. Polym. Sci.* **1969**, *13*, 1741−1747.
(56) Ren, Z.; Chen, G.; Wei, Z.; Sang, L.; Qi, M. Hemocompatibility Evaluation of Polyurethane Film with Surface-Grafted Poly(Ethylene Glycol) and Carboxymethyl-Chitosan. *J. Appl. Polym. Sci.* **2013**, *127*, 308−315.
(57) Pensa, N. W.; Curry, A. S.; Bonvallet, P. P.; Bellis, N. F.; Rettig, K. M.; Reddy, M. S.; Eberhardt, A. W.; Bellis, S. L. 3D Printed Mesh Reinforcements Enhance the Mechanical Properties of Electrospun Scaffolds. *Biomater. Res.* **2019**, *23*, 22.
(58) Kokubo, T.; Kushitani, H.; Sakka, S.; Kitsugi, T.; Yamamuro, T. Solutions able to reproducein vivo surface-structure changes in bioactive glass-ceramic A-W3. *J. Biomed. Mater. Res.* **1990**, *24*, 721−734.
(59) Mardirossian, M.; Pompilio, A.; Crocetta, V.; De Nicola, S.; Guida, F.; Degasperi, M.; Gennaro, R.; Di Bonaventura, G.; Scocchi, M. In Vitro and in Vivo Evaluation of BMAP-Derived Peptides for the Treatment of Cystic Fibrosis-Related Pulmonary Infections. *Amino Acids* **2016**, *48*, 2253−2260.
(60) Fujihara, K.; Kotaki, M.; Ramakrishna, S. Guided Bone Regeneration Membrane Made of Polycaprolactone/Calcium Carbonate Composite Nano-Fibers. *Biomaterials* **2005**, *26*, 4139−4147.
(61) Shao, J.; Yu, N.; Kolwijck, E.; Wang, B.; Tan, K. W.; Jansen, J. A.; Walboomers, X. F.; Yang, F. Biological Evaluation of Silver Nanoparticles Incorporated into Chitosan-Based Membranes. *Nanomedicine* **2017**, *12*, 2771−2785.
(62) Martins, A.; Pinho, E. D.; Faria, S.; Pashkuleva, I.; Marques, A. P.; Reis, R. L.; Neves, N. M. Surface Modification of Electrospun Polycaprolactone Nanofiber Meshes by Plasma Treatment to Enhance Biological Performance. *Small* **2009**, *5*, 1195−1206.
(63) Prado-Prone, G.; Silva-Bermudez, P.; Bazzar, M.; Focarete, M. L.; Rodil, S. E.; Vidal-Gutiérrez, X.; García-Macedo, J. A.; García-Pérez, V. I.; Velasquillo, C.; Almaguer-Flores, A. Antibacterial Composite Membranes of Polycaprolactone/Gelatin Loaded with Zinc Oxide Nanoparticles for Guided Tissue Regeneration. *Biomed. Mater.* **2020**, *15*, 035006.
(64) Marassi, V.; Di Cristo, L.; Smith, S. G. J.; Ortelli, S.; Blosi, M.; Costa, A. L.; Reschiglian, P.; Volkov, Y.; Prina-Mello, A. Silver Nanoparticles as a Medical Device in Healthcare Settings: A Five-Step Approach for Candidate Screening of Coating Agents. *R. Soc. Open Sci.* **2018**, *5*, 171113.
(65) Chambers, B. A.; Afrooz, A. R. M. N.; Bae, S.; Aich, N.; Katz, L.; Saleh, N. B.; Kirisits, M. J. Effects of Chloride and Ionic Strength on Physical Morphology, Dissolution, and Bacterial Toxicity of Silver Nanoparticles. *Environ. Sci. Technol.* **2014**, *48*, 761−769.
(66) Stojkovska, J.; Kostić, D.; Jovanović, Ž.; Vukašinović-Sekulić, M.; Mišković-Stanković, V.; Obradović, B. A Comprehensive Approach to in Vitro Functional Evaluation of Ag/Alginate Nanocomposite Hydrogels. *Carbohydr. Polym.* **2014**, *111*, 305−314.
(67) Nam, J.; Huang, Y.; Agarwal, S.; Lannutti, J. Materials Selection and Residual Solvent Retention in Biodegradable Electrospun Fibers. *J. Appl. Polym. Sci.* **2008**, *107*, 1547−1554.
(68) Radulescu, M.; Andronescu, E.; Dolete, G.; Popescu, R.; Fufă, O.; Chifiriuc, M.; Mogoantă, L.; Bălşeanu, T.-A.; Mogoşanu, G.; Grumezescu, A.; Holban, A. Silver Nanocoatings for Reducing the Exogenous Microbial Colonization of Wound Dressings. *Materials* **2016**, *9*, 345.